Transactions of the Korean Nuclear Society Spring Meeting
Jeju, Korea, May 16-18, 2018

Noise and patient dose analysis of intensity-modulated dental CBCT

Jinwoo Kim [a], Jonghee Yun [a], Seungwoo Ha [a], Ho Kyung Kim [a,b*]
[a]*School of Mechanical Engineering, Pusan National University, Busan 46241, Republic of Korea*
[b]*Center for Advanced Medical Engineering, Pusan National University, Busan 46241, Republic of Korea*
[*]*Corresponding author: hokyung@pusan.ac.kr*

1. Introduction

Cone-beam computed tomography (CBCT) is commonly used in oral and dentomaxillofacial imaging to support dental implants and orthodontic treatments [1,2]. The CBCT can provide two-dimensional cross-sectional images in any directions, and three-dimensional volume information [3]. Furthermore, it is typically known that the CBCT has the advantage of low patient dose compared to the conventional multidetector CT [4].

Despite of the low-dose characteristics of CBCT, however, cancer risks due to CBCT procedures are unavoidable [5]. In dental treatments, such as dental implants and orthodontics, even a single patient can be exposed to x-ray exposures several times if the CBCT scan is performed before, during, and after the treatment process. Consequently, the dental CBCT is not free from concerns on the overexposure issue; hence it is important to estimate the patient dose in the dental CBCT and manage it.

In this study, we have investigated the beam-intensity modulation (BIM) technique for the dose reduction in the dental CBCT. The BIM technique is an extension of the tube-current modulation (TCM) technique [6,7] including tube-voltage modulation, and we investigated whether or not it can reduce the patient dose without loss in image quality compared to the conventional CBCT scanning with a constant beam intensity.

For various BIM scenarios, we have analyzed the patient dose by using the Monte Carlo (MC) method and have also obtained experimentally the CBCT images for an anthropomorphic head phantom and investigated the noise performances according to the BIM scenarios.

2. Materials and Methods

2.1 Beam-intensity modulations

In this work, we have analyzed the patient dose distributions and the noise performances of the reconstructed tomographic images for several BIM scenarios as illustrated in Fig. 1. The BIM is an extension of the TCM technique, which modulates not only the tube current but also the tube voltage during the CBCT scan. As shown in Fig. 1(a), which is the reference BIM scenario, the tube current and voltage are fixed at constant values of 20 mA and 100 kVp, respectively. The other plots in Fig. 1 show the BIM scenarios designed in this study; they use relatively higher tube output (i.e., tube voltage times tube current) around the posterior side of the head, which includes the high-attenuating cervical spine. Note that each scenario has the same total beam intensity (i.e., the same area under each curve in the plots).

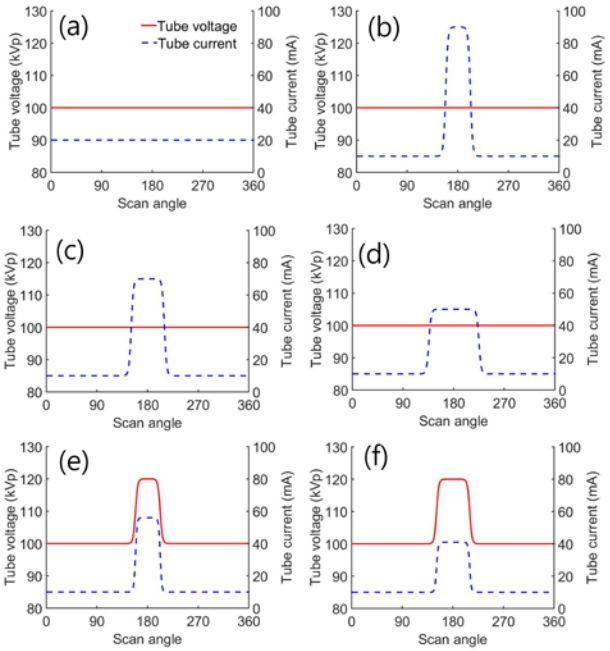

Fig. 1. Various beam-intensity modulation scenarios for the assessment of the noise-to-dose performances in dental CBCT. Scenario (a) is the reference. Scenarios (b), (c), and (d) modulate the tube current when the source traverses the posterior. Scenarios (e) and (f) modulate both the tube current and voltage.

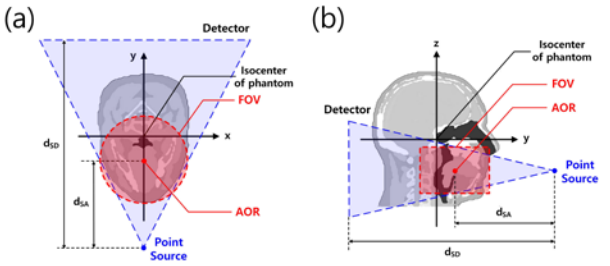

Fig. 2. The CBCT geometry for the MC simulations: (a) top view and (b) side view. The FOV, AOR, d_{SA}, and d_{SD} denote the field of view, axis of rotation, source-to-AOR distance, and source-to-detector distance, respectively.

2.2 Monte Carlo dose assessment

Patient dose assessment was performed by using the Monte Carlo N-Particle transport code (MCNP version 5, RSICC, Oak Ridge, TN, USA). The particle-tracking function of the MCNP was used to estimate the absorbed organ doses in the anthropomorphic numerical phantom

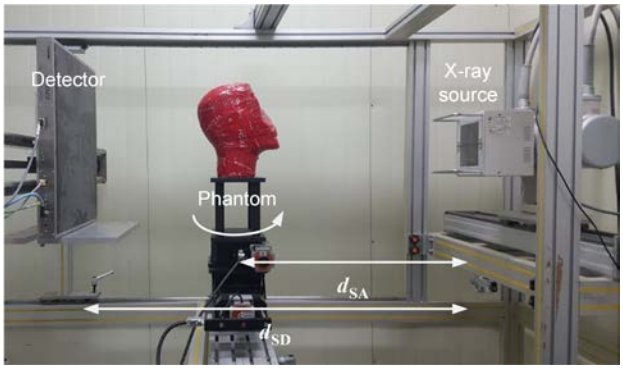

Fig. 3. A picture describing the developed bench-top CBCT system.

(XCAT version 2.0, Duke University, Durham, NC, USA).

The CBCT geometry for the MC simulations is shown in Fig. 2. The x-ray source rotates 360 degrees with the step angle of 1 degree, and a 130×80 mm-sized cylindrical field of view (FOV) that includes the maxilla and mandible is scanned. The source-to-axis of rotation distance (d_{SA}) and the source-to-detector distance (d_{SD}) are 450 and 630 mm, respectively.

2.3 Experimental

The bench-top CBCT system, as shown in Fig. 3, mainly consists of an x-ray source, an object stage, and an imaging detector and is based on the step and shoot operation. For image reconstruction, we use the well-known FDK algorithm [8].

To analyze the effect of the BIM technique on the tomographic image quality, we have evaluated image noise:

$$\sigma = \sqrt{(\mu - \bar{\mu})^2}, \quad (1)$$

where μ and $\bar{\mu}$ denote the pixel value and mean pixel value of the regions of interest (ROIs), respectively. The ROIs are selected at three regions: front, right side and center of the head (refer to Fig. 5(a)). As a figure of merit (FOM) for the BIM technique, we combine the measured noise and the effective dose that is assessed from the MC simulations:

$$\text{FOM} = {}^{1}/_{\sigma_{avg} \cdot E}. \quad (2)$$

3. Preliminary Results

Figure 4 shows the absorbed dose distribution for the reference (scenario (a)) and its subtractions with absorbed dose distributions obtained for various BIM scenarios. As shown in Fig. 4(a), the absorbed dose distribution shows a large dose concentration in the regions through which the x-ray beam is directly irradiated (i.e., beam path), and intense absorbed doses appear in the bone tissues such as maxilla, mandible, and cervical spine. The greatest difference between the absorbed dose distributions obtained for the reference and BIM scenarios can be observed in the beam path. Compared to the reference, the scenarios (b)-(d) and (e)-(f) reduce the effective dose by about 10% and 8%, respectively.

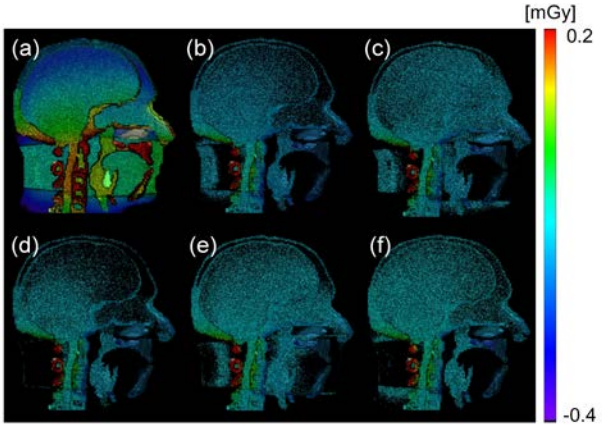

Fig. 4. The plot of (a) represents the absorbed dose distribution for the CBCT with the constant tube current and voltage (reference). The other plots of (b)-(f) show the absorbed dose distributions for various BIM scenarios correspondingly defined as in Figs. 1(b)-(f). Note that each distribution plot shows the subtraction images with the reference (a). The scale bar is read by the plots of (b)-(f).

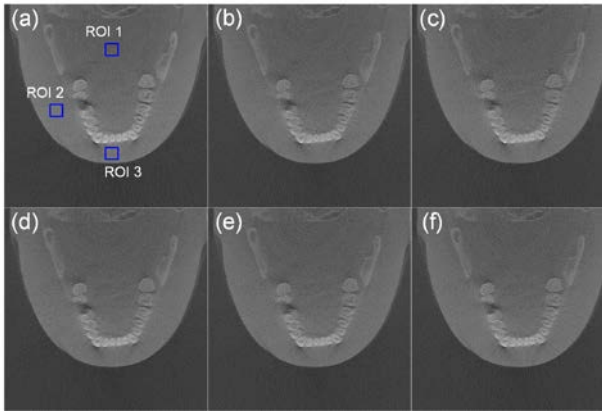

Fig. 5. The reconstructed images obtained for various BIM scenarios as defined in Fig. 2. The boxes designated in (a) represent the ROIs where the noise performances are evaluated.

Figure 5 represents the reconstructed images for various BIM scenarios. Compared to the reference, in the scenarios (b)-(d), which consider only tube-current modulation, it is observed that the noise performance is degraded by about 35%. On the other hand, in the scenarios (e) and (f), which considers the tube current and voltage modulations, the noise performance is slightly improved. Consequently, as shown in Fig. 6, scenario (f) records the best FOM due to the best noise performance and scenarios (b), (c), and (d) record worse FOMs than the reference.

4. Conclusion

The patient dose and the noise performance of the intensity-modulated dental CBCT have been analyzed. The conventional TCM technique showed a reduction effect in both absorbed organ doses and effective dose. However, it also degraded the image quality in terms of noise. Despite the slight contrast enhancement, the

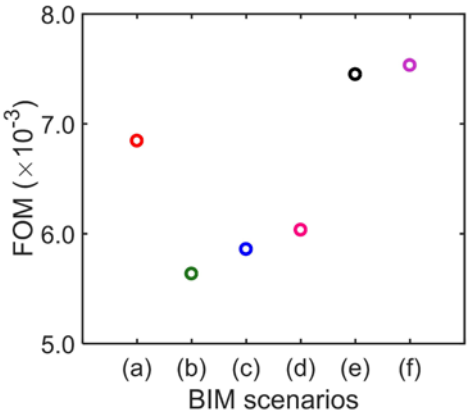

Fig. 6. The FOM for the corresponding BIM scenarios.

increase in noise was greater and this increased noise might make diagnostic performance low.

The current plus voltage modulating BIM technique is less effective for reducing patient dose, but it can improve the noise performance, so it is suitable for high quality imaging with low patient dose. In addition, more intensive tube output in the narrower section of the posterior side of the head is effective in reducing patient dose but it can also degrade the noise performance of the image.

ACKNOWLEDGEMENT

This work was supported by the National Research Foundation of Korea (NRF) grant funded by the Korea government (MSIP) (No. 2017M2A2A6A01071267).

REFERENCES

[1] W. C. Scarfe et al., “Clinical applications of cone-beam computed tomography in dental practice,” J. Can. Dent. Assoc. **72**(1), p. 75, 2006.
[2] J. A. Roberts et al., “Effective dose from cone beam CT examinations in dentistry,” Brit. J. Radiol. **82**(973), pp. 35–40, 2009.
[3] A. Miracle and S. Mukherji, “Conebeam CT of the head and neck, part 1: Physical principles,” Am. J. Neuroradiol. **30**(6), pp. 1088–1095, 2009.
[4] T. P. Cotton et al., “Endodontic applications of cone-beam volumetric tomography,” J. Endodont. **33**(9), pp. 1121 – 1132, 2007.
[5] D. J. Brenner and E. J. Hall, “Computed tomography - an increasing source of radiation exposure,” New Eng. J. Med. **357**(22), pp. 2277–2284, 2007.
[6] M. Gies et al., “Dose reduction in CT by anatomically adapted tube current modulation. I. simulation studies,” Med. Phys. **26**(11), pp. 2235–2247, 1999.
[7] W. A. Kalender et al., “Dose reduction in CT by anatomically adapted tube current modulation. II. phantom measurements,” Med. Phys. **26**(11), pp. 2248–2253, 1999.
[8] L. A. Feldkamp et al., “Practical cone-beam algorithm,” J. Opt. Soc. Am. A **1**(6), pp. 612–619, 1984.